ISTITUTO NAZIONALE DI FISICA NUCLEARE

Sezione di Catania

INFN/AE-04/12
23 November 2004

RECONSTRUCTION OF THE $K^*(892)^0$ RESONANCE SIGNAL IN pp COLLISIONS AT THE LHC REGIME THROUGH THE ALICE DETECTOR

Angela Badalà[1], Roberto Barbera[1,2]
Giuseppe Lo Re[3], Armando Palmeri[1] , Alberto Pulvirenti[1,2]
Giuseppe S. Pappalardo[1] and Francesco Riggi[1,2]
[1)]INFN-Sezione di Catania, Italy
[2)]Dipartimento di Fisica e Astronomia, Università di Catania,, Italy
[3)]CNAF, Bologna, Italy

Abstract

The reconstruction of the physics signal due to the decay of $K^*(892)^0$ and its antiparticle into $K\pi$ in pp collisions at the energetic regime planned for the Large Hadron Collider (LHC) has been investigated by a full simulation carried out within the environment of the ALICE detector. The event mixing technique was used to evaluate the combinatorial background. The role of particle identification of the decay products is discussed. Detection efficiency and statistical significance are reported.

PACS.: 13.25.Es, 25.75.+r

Published by ***SIS–Pubblicazioni***
Laboratori Nazionali di Frascati

1 INTRODUCTION

The study of resonances which have lifetimes comparable to that of the dense matter created in heavy-ion collisions at ultrarelativistic energies is an important tool to have information on the collision dynamics. Modifications of the properties of such resonances and of their production rate may be expected when they are produced in a dense medium. The study of such resonances, compared to that of other particles produced in the collision, may also probe the role of the rescattering phase between chemical and kinetic freeze-out. Since these resonances may decay still in the hot hadronic matter, rescattering of the daughter particles may take place, depending on the source size and lifetime, as well as on the parent transverse momentum. Finally, the combined investigation of resonances with strange quark content, as the $K^*(892)^0$ and $\Phi(1020)$ mesons, is also important due to the expected overall strangeness enhancement in heavy-ion collisions.

The study of strange particles (K^0_s, Λ) as well as of the cascades (Ξ and Ω) and of the $\Phi(1020)$ signal was carried out within the ALICE Collaboration[1,2]. As far as the production of rare meson resonances is concerned, no detailed simulation was reported so far. The observation of such resonances is critical in heavy-ion experiments, due to the large background originating from the high multiplicity and from detector limitations. Among the more recent results, the NA49 Collaboration has reported an experimental study of the $\Phi(1020)$, $K^*(892)^0$ and $\Lambda(1520)$ in Pb+Pb at 158 AGeV through their hadronic decay channels[3]. Significant results on the production of $K^*(892)^0$ and its antiparticle were reported by the STAR Collaboration in Au+Au central collisions at $\sqrt{s}$=130 GeV[4] and 200 GeV[5], where transverse mass spectra, yields and particle ratios were extracted from the data.

The possibility to identify and correctly reconstruct the decay kinematics of such resonances will be of great interest at the energetic regime planned for the Large Hadron Collider (LHC), where the high multiplicity environment expected for Pb+Pb collision at 5.5 ATeV will pose a dramatic challenge to any tracking and reconstruction procedure.

Preliminary results concerning the reconstruction of the high-pt signal due to $K^*(892)^0$ decay in Pb-Pb collisions have been reported within the ALICE Collaboration[6]. Here a simulation study of the $K^*(892)^0$ signal in pp collisions is discussed, taking into account the present status of the detector and the available reconstruction algorithms. First results on this topic were published in the Proceedings of the ACAT 2003 Conference[7].

The large amount of events (in the order of several 10^5 for pp) and computer resources needed for such investigation brought us to consider the use of the AliEn GRID middleware ALIEN[8], the ALICE package for distributed computing.

Typical results from such investigation will be presented, including the reconstruction procedure for the $K^*(892)^0$ resonance, the improvement of the signal-to-background ratio by means of kinematical cuts, and the role of particle identification in the ALICE environment.

Sect.II briefly reports some basic information concerned with the ALICE detector, especially its main tracking devices, while Sect.III is concerned with the software simulation and reconstruction chain in ALICE. Sect.IV discusses the reconstruction procedure of the $K^*(892)^0$ decay, and typical results which may be obtained with and without the particle

identification information. Some comments concerning possible improvement of the detection strategy in the near future are made in Sect. V.

2 THE ALICE DETECTOR

The ALICE detector[9] will be used in one of the large experiments planned at the future CERN Large Hadron Collider (LHC). It will be optimized for the study of heavy-ion collisions at a c.m. energy of 5.5 TeV per nucleon, to cope with the large particle multiplicities expected from such collision events. Fig.1 shows the layout of the ALICE detector. It includes two main components: a central barrel, placed in the magnetic field of the L3 magnet, and a forward muon spectrometer. The central barrel consists of several concentric layers of detectors: the Inner Tracker System (ITS)[10], the Time Projection Chamber (TPC)[11], the Transition Radiation Detector (TRD)[12] and the Time-Of-Flight system (TOF)[13]. The coverage of the central barrel allows the tracking of particles emitted with a pseudorapidity between -0.9 and 0.9, with full azimuthal acceptance and with a very low p_t threshold.

The forward muon spectrometer[14] covers the pseudorapidity range between 2.4 and 4, and makes use of a front absorber, a dipole magnet, a set of muon tracking chambers, a muon filter and four trigger chambers.These large area detectors are complemented by other, smaller area detectors for high-momentum identification, photon detection, charged particle multiplicity information and trigger.

The present study makes use of the information available from the two inner detectors, the ITS and the TPC, which have good tracking capabilities even in presence of events with a large particle multiplicity, and allow for the reconstruction of charged particle tracks with optimal impact parameter and momentum resolution.

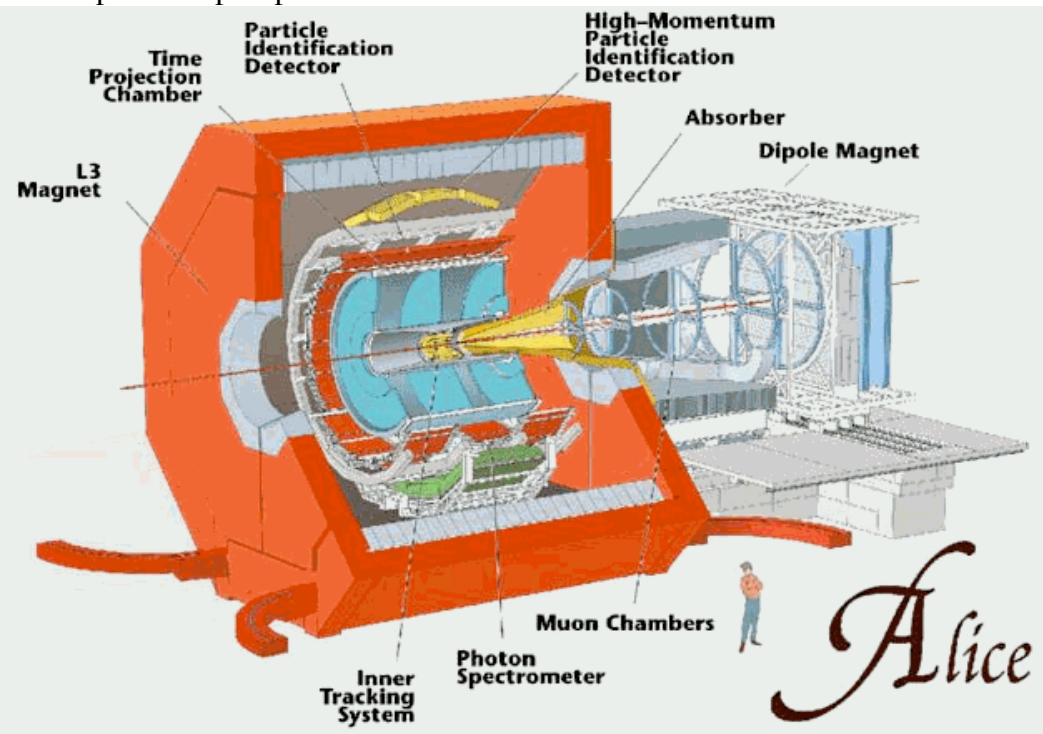

FIG. 1: Schematic view of the ALICE detector.

3 THE ALICE SIMULATION AND RECONSTRUCTION ENVIRONMENT

The general framework AliRoot[15] for the simulation and reconstruction in the ALICE detector has been used in this study. The role of this framework is to generate physics events according to one of the existing event generators, simulate the interaction of primary and secondary particles with the detectors, taking into account the geometry and detector response, produce raw data and implement all the strategy for the reconstruction chain. I/O and user interface are part of this framework, together with data visualization and any analysis tool. A large effort has been made in order to ensure modularity and reusability of the code.

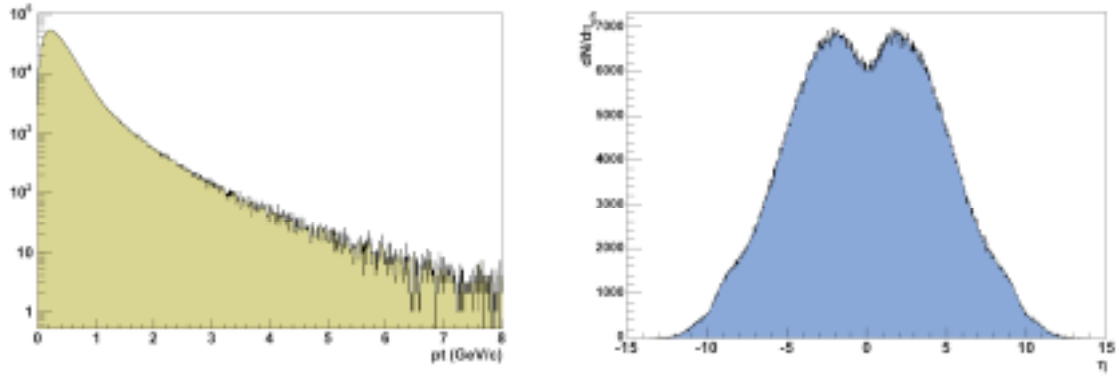

FIG. 2: Charged particle transverse momentum (left) and pseudorapidity (right) distributions from the PYTHIA event generator for pp collisions at √ s=14 TeV.

Several event generators have been used within the AliRoot framework, depending on the physics to be studied. For pp collisions, both the PYTHIA[16] (Version 6.203) and Herwig[17] (Version 6.1) codes are currently used. The PYTHIA generator, which was used in the present study, is based on perturbative QCD, but also includes models of soft interactions, parton showers and multiple interactions, fragmentation and decays. Fig. 2 shows the charged particle pseudorapidity and transverse momentum distributions produced in minimum bias pp collisions at √(s) = 14 TeV, while Fig.3 shows the charged particle multiplicity distribution.

The tracking strategy inside the main ALICE tracking devices, the ITS and the TPC, is currently based on the use of a Kalman filter procedure, as originally used by P.Billoir[18]. While still in progress to improve some aspect, the present tracking algorithms already provide a good track finding efficiency, impact parameter and momentum resolution down to p_t=100 MeV/c, even for large track densities as it is the case in Pb-Pb collisions.

Analysis tools are also being developed within the common AliRoot framework, for the investigation of detector performance and for the study of physics signals.

Recently a distributed computing environment, named AliEN[8] (Alice ENvironment) has been developed by the ALICE Collaboration to provide a transparent access to worldwide distributed computer resources and data files. These technologies are associated with the Grid philosopy[19].

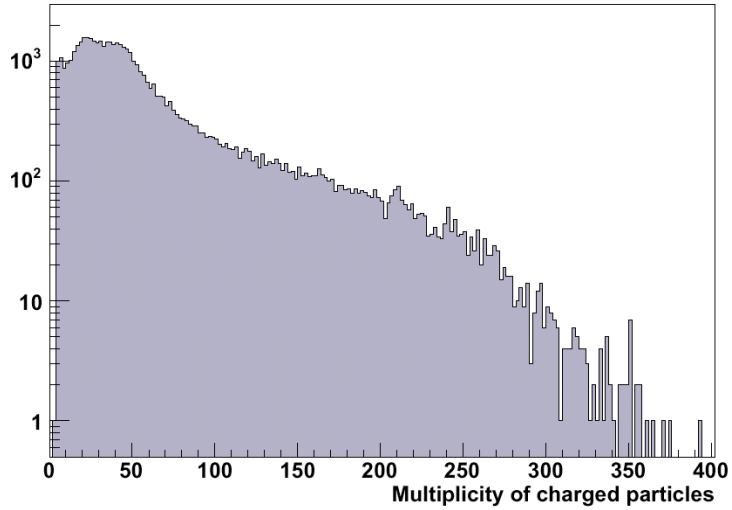

FIG. 3: Multiplicity distribution of the particles generated by PYTHIA for pp collisions at √ s=14 TeV.

Currently, AliEn is being used for the distributed production of Montecarlo data, detector simulation and reconstruction. For the present study we used the AliEn environment to generate and fully analyze about 200000 pp events using data files and computer resources distributed in several sites, in a user-transparent mode. More details on the procedure and performance of this approach are given elsewhere[7].

4 RECONSTRUCTION OF THE $K^*(892)^0$ SIGNAL

The $K^*(892)^0$ meson resonance and its antiparticle decay into $K\pi$, with a $c\tau$ around 4 fm/c and full width Γ = (50.7 ± 0.6) MeV. Their decay products may therefore be considered as primary particles as far as the tracking is concerned. This is a big problem when dealing with the huge multiplicity expected in Pb-Pb collisions, whereas the problem is relatively easier in case of pp collisions. The selection of the $K^*(892)^0$ decay channel into charged particles may be achieved in principle by the invariant mass analysis with some selection of kinematical cuts to improve the signal-to-background ratio.

For this study we generated and fully analyzed PYTHIA pp minimum bias events at √ s= 14 TeV. A magnetic field B=0.4 T inside the ALICE magnet was chosen.

These events are basically the input for our simulation. Particles were considered over the whole solid angle and in the full momentum range. All of the ALICE subdetectors, together with the beam pipe, were included in the simulation, and all physical processes were switched on in GEANT. In the reconstruction process, space points for each track were evaluated by a full treatment of the ITS and TPC response.

The average $K^*(892)^0$ multiplicity, as generated by PYTHIA, is in the order of 1.7 per event (3.4 for $K^*(892)^0$ and antiparticle), whereas the number of possible $K^+\pi^-$ combinations is in the order of 70 per event.

Several factors need to be taken into account in order to understand the actual number of $K^*(892)^0$ candidates which are findable after the reconstruction process. The geometrical acceptance of the TPC ($-0.9 < \eta < 0.9$), the branching ratio of the $K^*(892)^0$ decay into $K^+\pi^-$ and the tracking efficiency, especially for low momentum particles originating from the resonance decay and for the charged kaons which in turn decay inside the TPC volume, are all factors which strongly reduce the number of findable candidates, to about 0.02 per event. After tracking, the $K^+\pi^-$ combinations are reduced to about 1.4 per event.

4.1 Ideal mass identification

To start with, we assumed a perfect knowledge of the particle identification. The effect of misidentifying the decay products will be discussed later in this paper. In such a condition, the true signal which could be obtained from a proper correlation of the true pairs is shown in fig.4 (left). A fit of such peak gives a centroid at (897.4 ± 1.0) MeV, and a width of (53.7 ± 2.4) MeV, which are compatibile with the standard values reported by the PDG group[20]. Both $K^*(892)^0$and its antiparticle were included in the plot, by summing $K^+\pi^-$ and $K^-\pi^+$ pairs.

The decay products from the $K^*(892)^0$ are embedded in a sample of primary tracks, with a signal-to-background ratio S/B = 0.1 within 2 σ with respect to the nominal $K^*(892)^0$ invariant mass (fig.4, right). The significance $S/\sqrt{(S+B)}$ is 11.1 for the actual number of events considered in the present analysis.

Only a soft kinematical cut on the relative angles of the two daughter momenta α_π, α_K, with respect to the parent momentum was introduced ($\alpha_\pi < 1$ rad, $\alpha_K < 2$ rad), which results in a signal-to-background ratio S/B = 0.102 and a significance of 11.1, with a reconstruction efficiency of about 98 %. The number of $K^*(892)^0$ per event amounts to 0.018 with such cut.

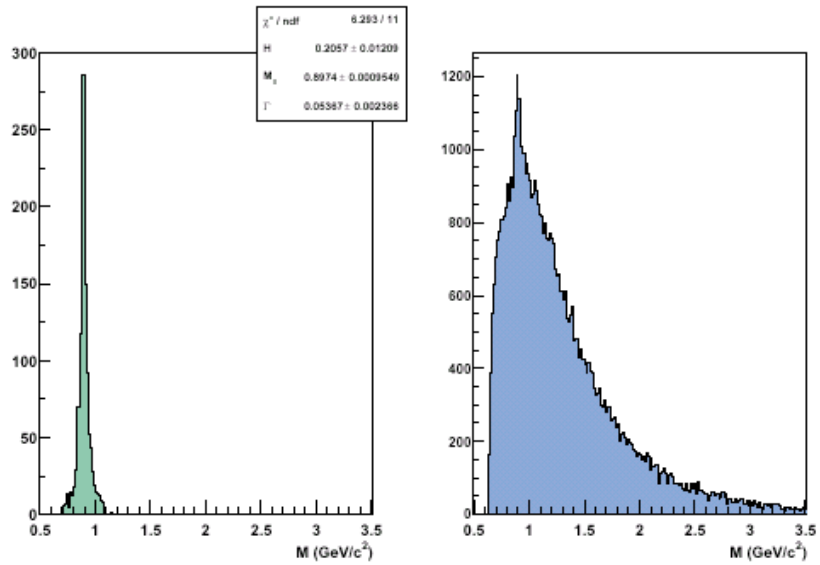

FIG. 4: Invariant mass distribution of the true pairs originating from the $K^*(892)^0$ and its antiparticle decay (left) and from all pairs (right).

The effect of other possible kinematical cuts on the variables of interest, such as the impact parameter of the two tracks, their χ^2, the closest distance between the two tracks and the transverse momenta of the two daughters was also investigated, but it was checked not to give any sensitive improvement on the ratio S/B.

A fit of the signal spectrum (fig.4, right) carried out with the sum of a polynomial and a Breit-Wigner shape, gives a centroid at (894.9 ± 2.4) MeV and a width Γ = (59.1 ± 11.6) MeV for the $K^*(892)^0$ peak, which are still compatible, although with a large uncertainty in the width, with the nominal values.

We also checked the effect of introducing a cut in the Armenteros-Podolanski plot. This technique[21] is a very useful method to analyze the decay of a parent particle into two tracks with opposite charge. It is based on the plot, for each event, of the transverse component of one of the two decay product's momenta with respect to the parent direction (q_t) against the quantity $\alpha = (q_{L+} - q_{L-}) / (q_{L+} + q_{L-})$, where q_{L+} and q_{L-} are the components of momenta of the positive and negative tracks parallel to the parent direction. Decay pairs originating from a given parent will fall into an elliptical locus, with the axes of the ellipse dependent on the masses of the parent and the decay products. While a strong cut around the ellipse will have a similar effect as a mass cut, the Armenteros-Podolanski plot may be used to distinguish different parents when particle identification is not available, or to improve with a soft cut the signal-to-background ratio, eliminating some region of the (α, q_t) plane, where the contribution of uncorrelated particle pairs may be relatively large.

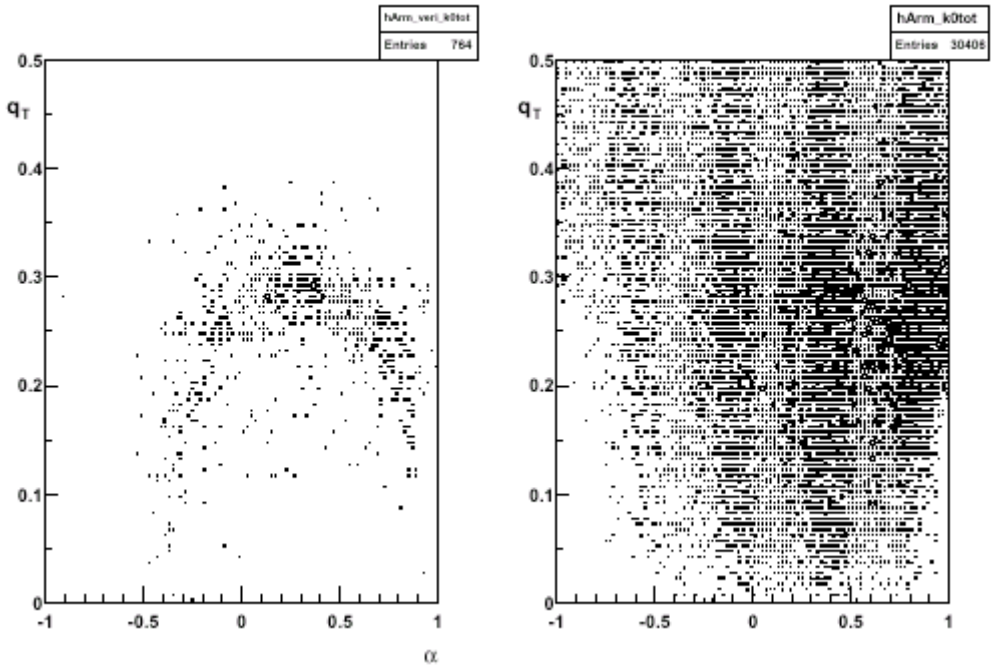

FIG. 5: Armenteros-Podolanski scatter plot of the true pairs originating from the $K^*(892)^0$ decay (left) and from all identified $K^+\pi^-$ pairs (right).

For the $K^*(892)^0$ decay into $K^+\pi^-$, the equation of the elliptical kinematical locus is given by

$$\frac{(\alpha - \lambda)^2}{\alpha^{*2}} + \frac{q_t^2}{q^{*2}} = 1$$

with semiaxes α^* and q^*, where $\alpha^* = 2q^*/(\beta\, m_a)$ (β is the velocity of the parent particle in the lab frame and m_a its mass) and q^* is the maximum momentum of the decay products. The center of the ellipse is located at $(\Lambda, 0)$, where $\Lambda = (E^*_+ - E^*_-)/ m_a$ and $E^*_\pm = [(q^*)^2 + m_\pm^2]^{1/2}$, m_+ and m_- being the masses of the positive and negative particles. For the $K^*(892)^0$ decay, $\alpha^* = 0.65$, $q^* = 0.291$ GeV/c, $\Lambda = 0.279$.

The Armenteros-Podolanski scatter plot for the $K^*(892)^0$ decay into $K^+\pi^-$ is shown in the left part of Fig.5, while the corresponding plot for all the $K^+\pi^-$ pairs is shown in the right part of Fig.5. A rectangular cut

$$-0.12 < \alpha < 0.67 \qquad\qquad 0.25 < q_t < 0.33$$

was chosen, which gives on the invariant mass spectrum, a signal-to-background ratio S/B= 0.146, with a significance of 8.9. For the antiparticle, symmetrical values of α were chosen.

The fit parameters of the resonance peak and their errors are comparable to those reported before.

These results show that with a perfect particle identification, the $K^*(892)^0$ signal may be extracted even with a limited number of events. A large improvement in the reliability of the fit parameters giving the yield and the width of the $K^*(892)^0$ signal may then be expected, due to the large statistics which can be achieved for pp collisions in a short time.

4.2 Missing mass identification

Charged particle identification (PID) is an ongoing task in ALICE, involving the combined information from several detectors (ITS, TPC, TOF and TRD). Several approaches are in principle possible, trying to have a good PID in a momentum interval as large as possible.

One approach is based on the separation which can be achieved for different particles by the use of suitable information from a detector, while the other evaluates the probability for each particle to be for instance a pion, a kaon or a proton considering the dE/dx distribution of all these particles.

A combined probability approach, which makes use of the information originating from all relevant detectors, is presently investigated. Here we checked the possibility to correctly reconstruct the $K^*(892)^0$ signal in pp collisions even in absence of any particle identification. This hypothesis largely underestimates the performance which may be actually

achieved by a proper use of the energy loss and TOF information and has the only meaning of exploring the worst possible scenario.

Without any information on the particle mass we have to consider all possible positive/negative pair combinations arising from $(\pi^+, K^+, p) \otimes (\pi^-, K^-, pbar)$.

The invariant mass spectrum corresponding to such a situation is shown in fig.6 (right). Clearly visible is the broad mass peak corresponding to the ω(770) and ρ(782) mesons (from $\pi^+ + \pi^-$ pairs), the contribution from Φ(1020), Λ and Δ(1232), together with a continuous background arising from particles which have a large branching ratio for three body decay, where only two of the three tracks are combined together. Fig.6 (left) shows, for comparison, the true $K^*(892)^0$ signal.

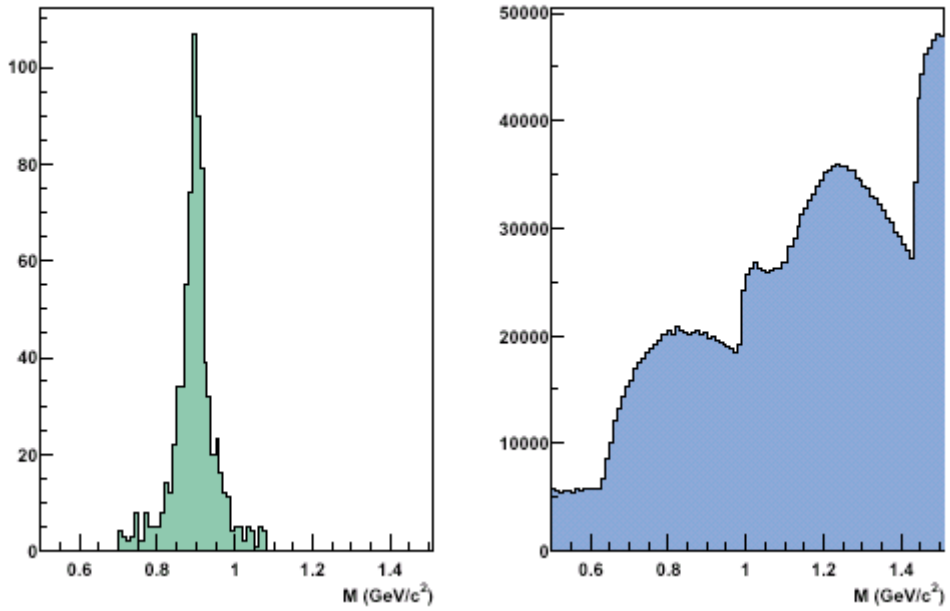

FIG. 6: Invariant mass distribution of all possible positive/negative pair combinations of pions, kaons and protons (right). On the left the true $K^*(892)^0$ signal is shown for comparison.

In order to reduce the effect of the pair combinations originating from resonances which result in a final state different from π K, we evaluated the Armenteros kinematical loci for all the relevant resonances which may contribute in this invariant mass region. Such curves are plotted in fig.7.

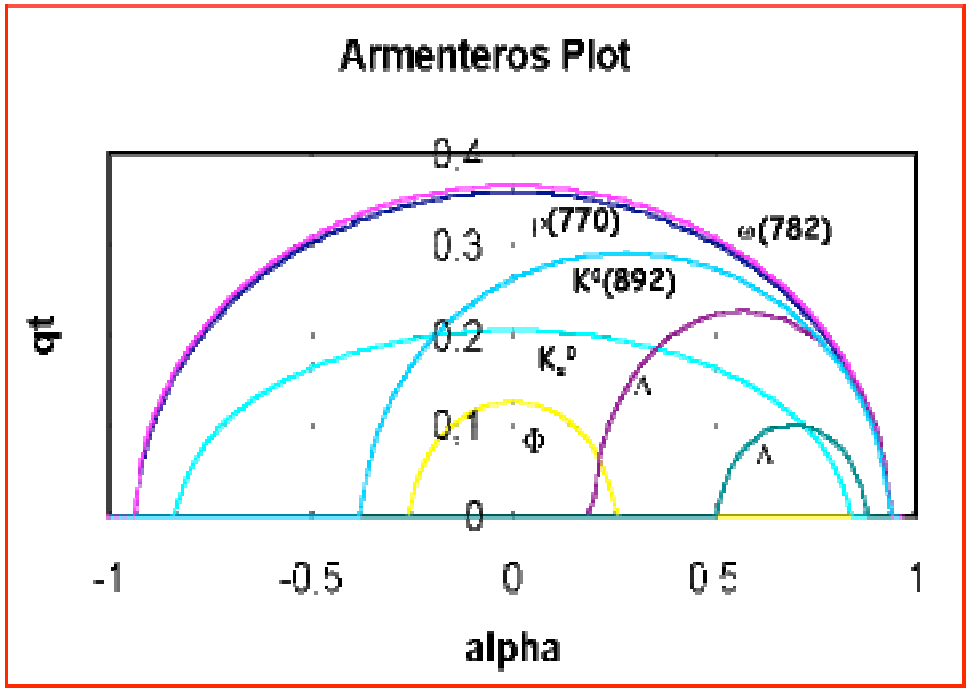

FIG. 7: Armenteros-Podolanski nominal curves for the resonances which may contribute to the invariant mass region around the $K^*(892)^0$ peak. For clarity, the kinematical loci of the corresponding charged antiparticles are not drawn.

As it can be seen, a large contribution within the rectangular area selected by the previous limits (Sect.4.1) comes from the ω (770) and ρ(782) mesons, whereas the contribution of Λ, Φ(1020) and Δ lie outside the selected limits. In this case a slightly stronger cut was used ($-0.12 < \alpha < 0.67$, $0.25 < q_t < 0.30$ for the $K^*(892)^0$ and symmetrical values of α for the antiparticle). We also added a cut on the minimum momentum of the decay kaon at 1.6 GeV/c. An additional condition may be inserted imposing that the invariant mass of the selected pair has to be different, within certain limits, from that of the two meson resonances: $| m_{inv} - m_\omega | < \varepsilon_\omega$, $| m_{inv} - m_\rho | < \varepsilon_\rho$. Several checks were made with different values of ε_ρ , due to the width of this resonance (Γ=150 MeV). A final value of 50 MeV was chosen.

Since the width of the ω(770) is Γ = 8.4 MeV the corresponding cut is not relevant, due to the imposed cut on the ρ(782).

With these conditions, an invariant mass spectrum as in fig.8 is obtained.

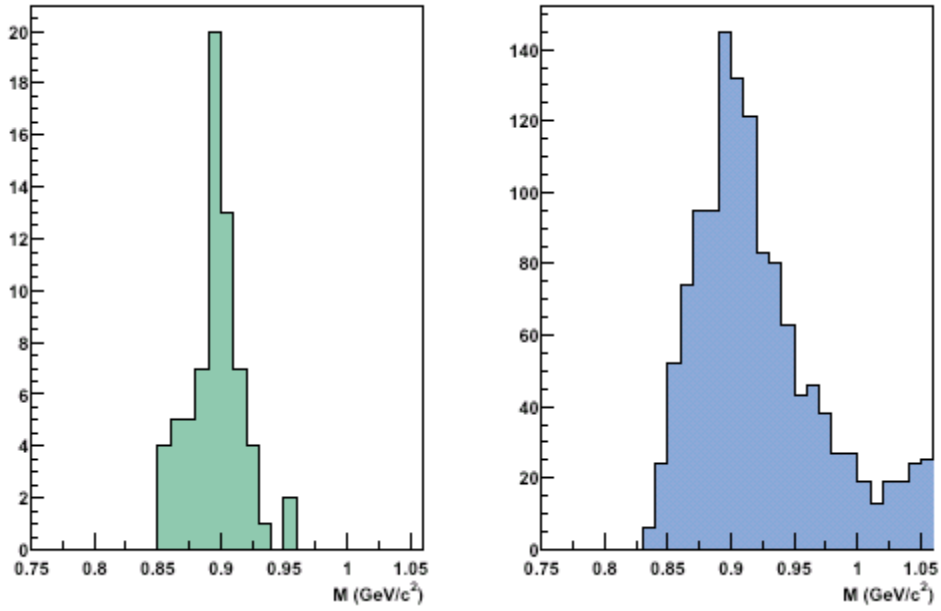

FIG. 8: Invariant mass spectrum (right) obtained without any particle identification on the decay products, after applying the cuts discussed in the text. For comparison, the true signal with the same cuts is shown on the left side.

Even with such cuts, a large background is still present in the mass region of interest, with a signal-to-background ratio S/B as small as 0.06. To subtract the combinatorial background, we built the mixed event spectrum by randomly choosing a couple of events in the data file and taking a particle from one event and the other particle from the other event. All (π, K, p) combinations were considered, similarly to what is done to build up the signal spectrum within the same event.

The number of event pairs was chosen as to to have a negligible statistical error on the combinatorial spectrum. Since the multiplicity fluctuations in pp collisions may be relatively large (see fig.3), a more correct procedure would be to mix only events which have comparable multiplicities. In our case we verified by the Kolmogorov test that the two procedures give very similar combinatorial spectra when event pairs whose multiplicities differ not more than 5 units are considered (see fig.9).

According to this prescription, the combinatorial spectrum was normalized to the same area of the signal spectrum (fig.10, left). The difference spectrum is shown in fig.10 (right). It manifests the expected positive-negative-positive pattern, due to the normalization to the same area[22]. A clear surplus of events is seen around the nominal $K^*(892)^0$ mass.

To extract the signal intensity and width, a fit of the spectrum was carried out with a procedure similar to that discussed in Sect.4.1. The result was a centroid at (0.895 ± 0.002) GeV, with a width Γ= (59 ± 11) MeV.

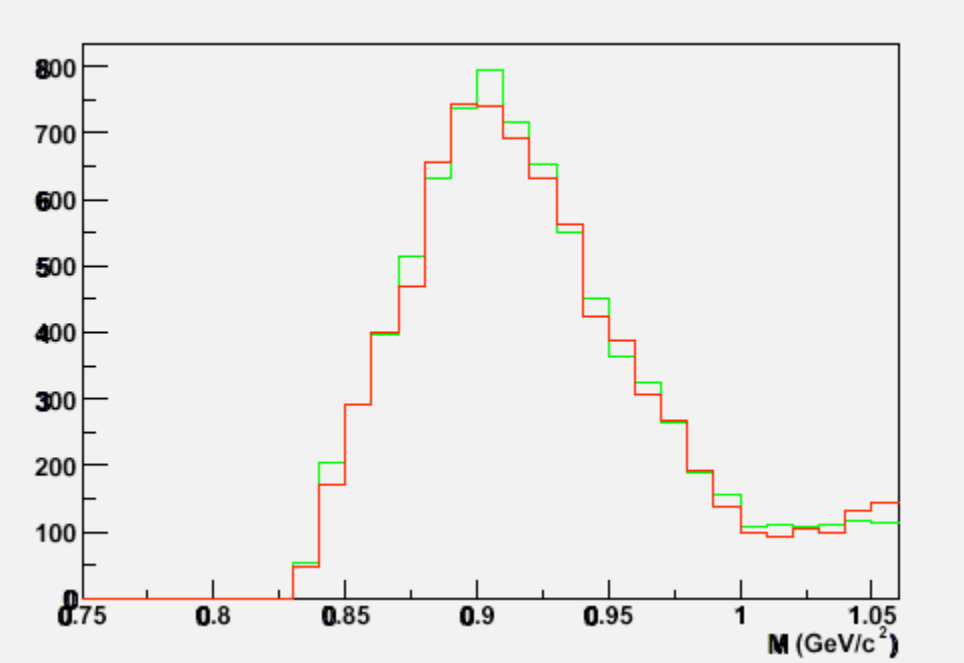

FIG. 9: Comparison between the combinatorial invariant mass spectrum built with any possible event pair and with only those event pairs which have multiplicities differing not more than five units.

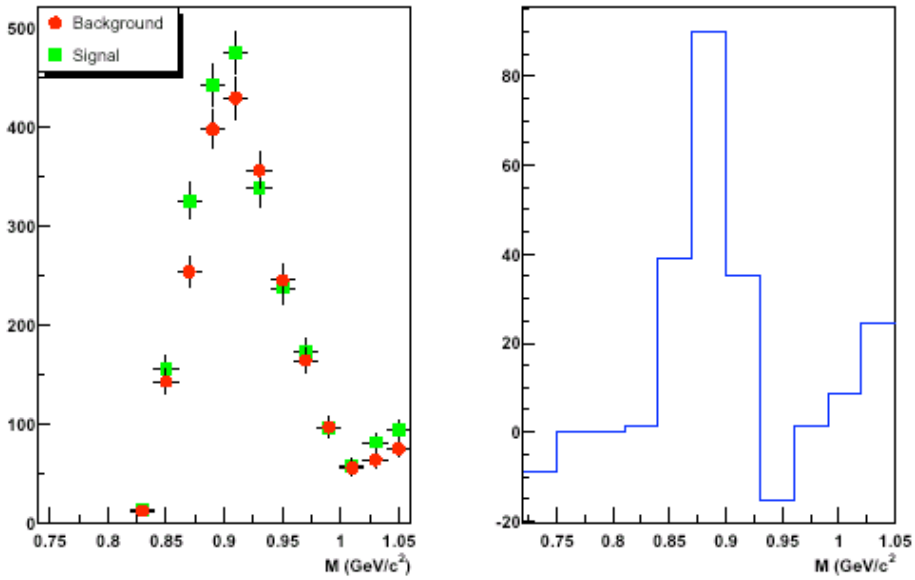

FIG. 10: Signal spectrum and combinatorial spectrum of $K^+\pi^-$ pairs from pp collisions (left), normalized to the same area (see text). The difference spectrum is shown on the right.

4.3 Present status of mass identification in ALICE

In this subsection we want to investigate the role of realistic particle identification (PID) in the ALICE detectors, according to the procedures currently used. Concerning PID, two cases were considered. In the first case, only one PID information was required, to maximize the number of tracks, while in the second case, PID information was required by all three detectors (ITS, TPC and TOF).

4.3.1 Particle identification: At least one PID, Case I

In this case, the PID information was required from at least one of the three detectors: ITS, TPC and TOF. Fig.11 shows the PID efficiency for all the tracks, while figs.12 and 13 show the same quantity for the kaons (fig.12) and for only the kaons originating from the resonance decay (fig.13). Table I show some numerical detail concerning the number of good and fake tracks for each species.

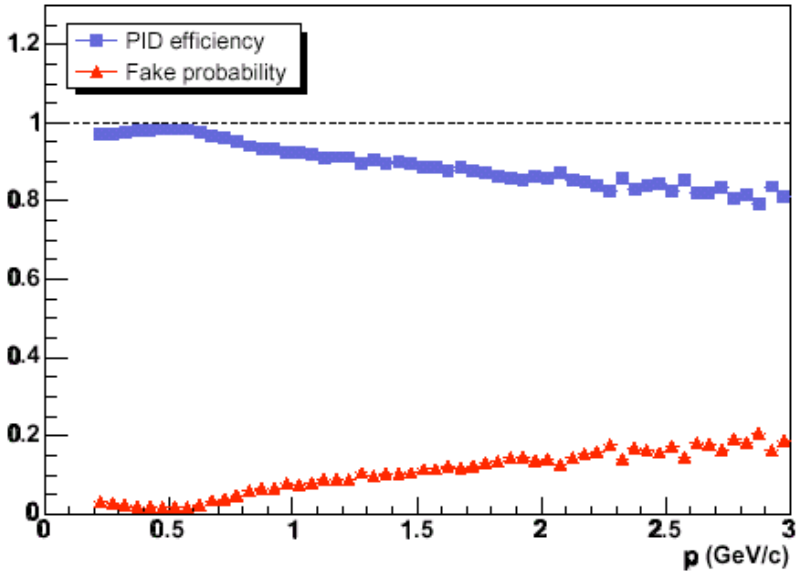

FIG. 11: The two plots show the PID efficiency and the fake probability as a function of the track momentum. The PID efficiency is defined as #identified tracks/#tracks and the fake probability as #missidentified tracks/#tracks.

TAB. 1: Summary of ALICE PID capability

	No. of tracks	No. of guessed tracks	Guessed (%)	No. of fake tracks	Fakes (%)
All	895528	853790	95.4	41738	4.7
π	780027	770716	98.8	9311	1.2
K	59683	45164	75.7	14519	24.3
P	42704	37910	88.7	4794	11.2
K from $K^{*}(892)^{0}$	19828	15303	77.1	4525	22.8

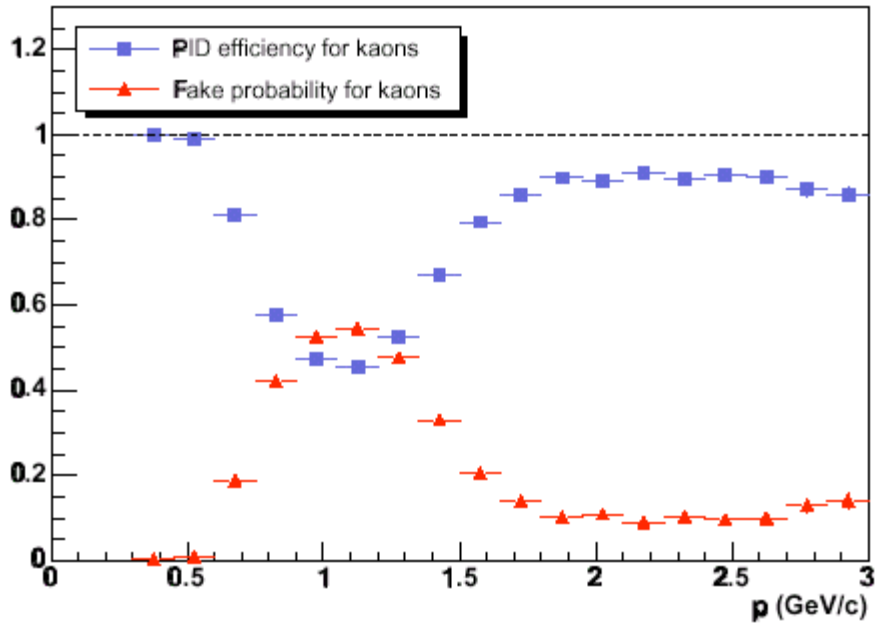

FIG. 12: As Fig.11, but for kaons only.

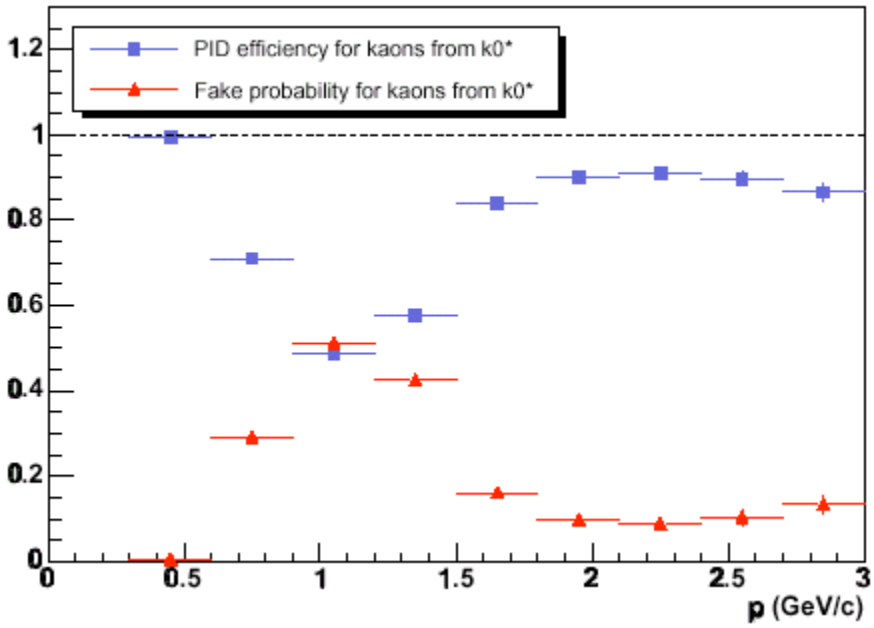

FIG. 13: As Fig.11, but only for kaons produced in the $K^*(892)^0$ decay .

For the $K^*(892)^0$ some numbers are the following: The number of findable $K^*(892)^0$ is 3947 (0.02/ev). A $K^*(892)^0$ is denoted as findable if both its two daughters have been tracked. The number of good $K^*(892)^0$ is 3008 (0.015/ev). A $K^*(892)^0$ is defined as good if both its two daughters have been tracked and correctly identificated. Considering the interval of invariant mass (0.8,1.0) in our case there are 2793 findable $K^*(892)^0$ among 36978 $K^+\pi^-$ combinations, with a signal to noise ratio S/B= 0.08 and a significance of 14.5 (Fig.14).

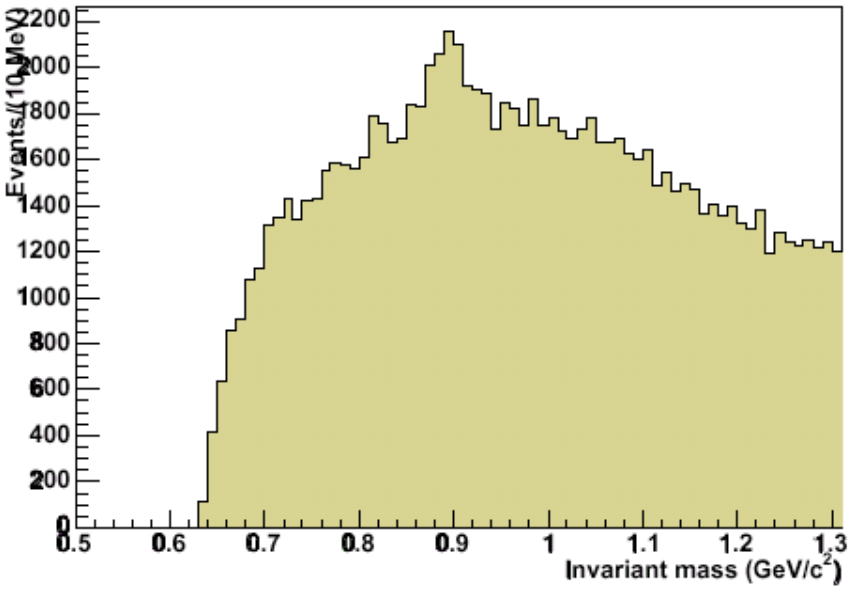

FIG. 14: Invariant mass distribution of the $K^+\pi^-$.

Fig.15 shows the invariant mass distribution of the true pairs, together with the contribution originating from other resonances which may contribute in the same mass region.

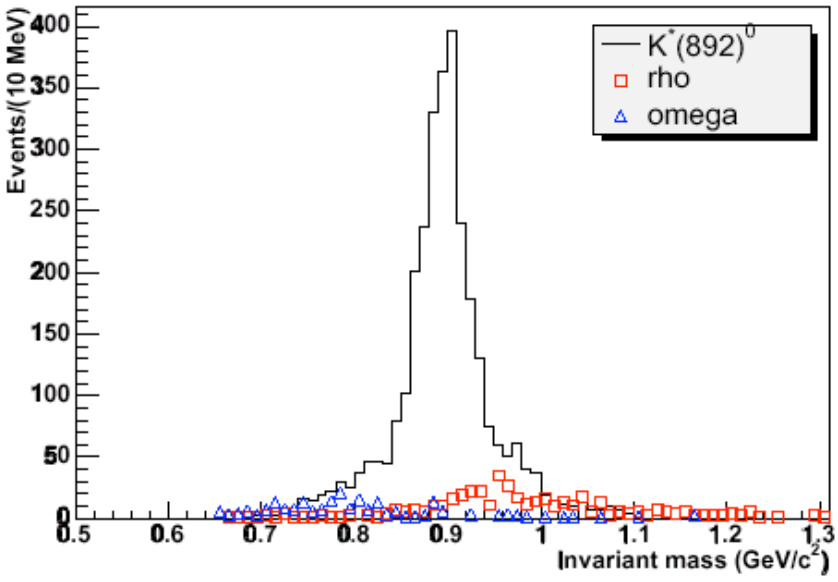

FIG. 15: Invariant mass distribution of the true $K^+\pi^-$ (black line), together with the individual contribution of the resonances which contribute in the same mass region.

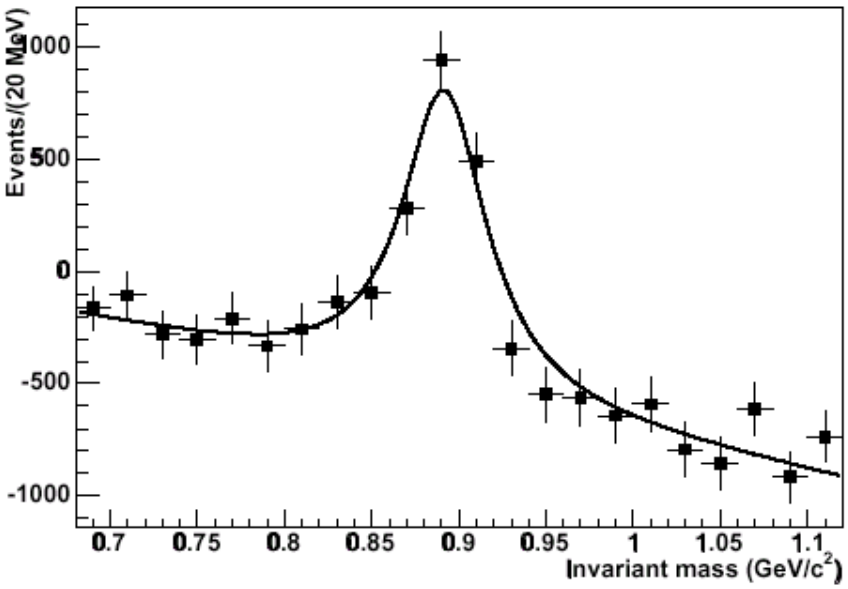

FIG. 16: Subtraction of the Kπ invariant mass distributions (both the $K^+ \pi^-$ and the $K^- \pi^+$ combinations have been included) and the mixed event background normalized to the same area. The resulting spectrum has been fitted with a Lorentzian curve plus a linear background. The fit results are M=(891 ± 2) MeV/c^2 and Γ=59 MeV/c^2.

The background was evaluated by the event mixing technique and subtracted from the Kπ invariant mass distribution. Both the $K^+\pi^-$ and the $K^-\pi^+$ combinations have been included. The mixed event spectrum was normalized to the same area. The resulting spectrum (Fig. 16) has been fitted with a Lorentzian curve plus a linear background. The fit results are M=(891 ± 2) MeV/c^2 and Γ = 59 MeV/c^2.

No further cut was introduced for the selection of events. Figs.17 and 18 show that the overall distributions of kaons and the distributions of those kaons originating from the $K^*(892)^0$ decay are very similar. Fig.19 shows the multiplicity spectrum of all the events and of those events containing a kaon from the $K^*(892)^0$ decay.

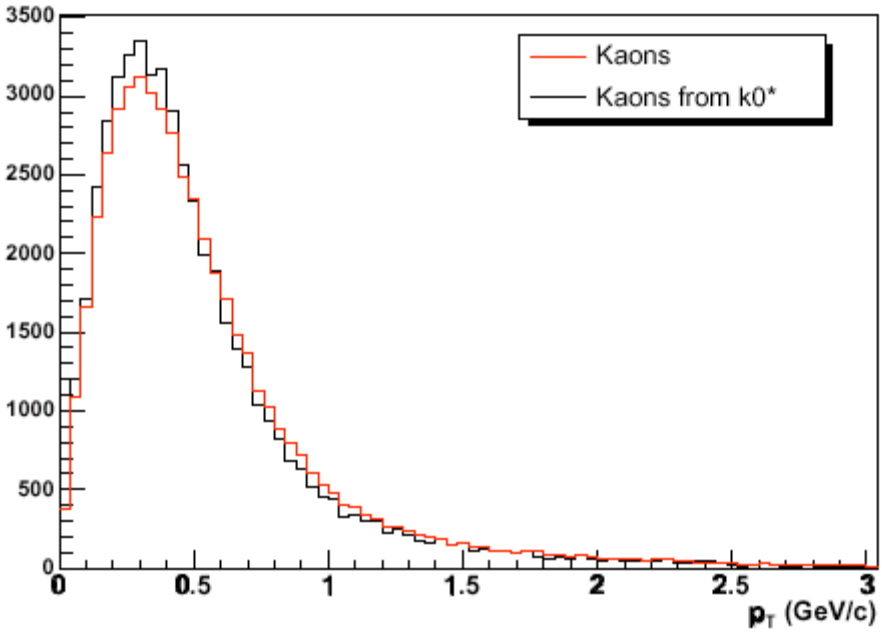

FIG. 17: p_t distribution of all kaons generated by PYTHIA (red), compared to that of the kaons produced in a $K^*(892)^0$ decay. The two spectra are normalized to the same area.

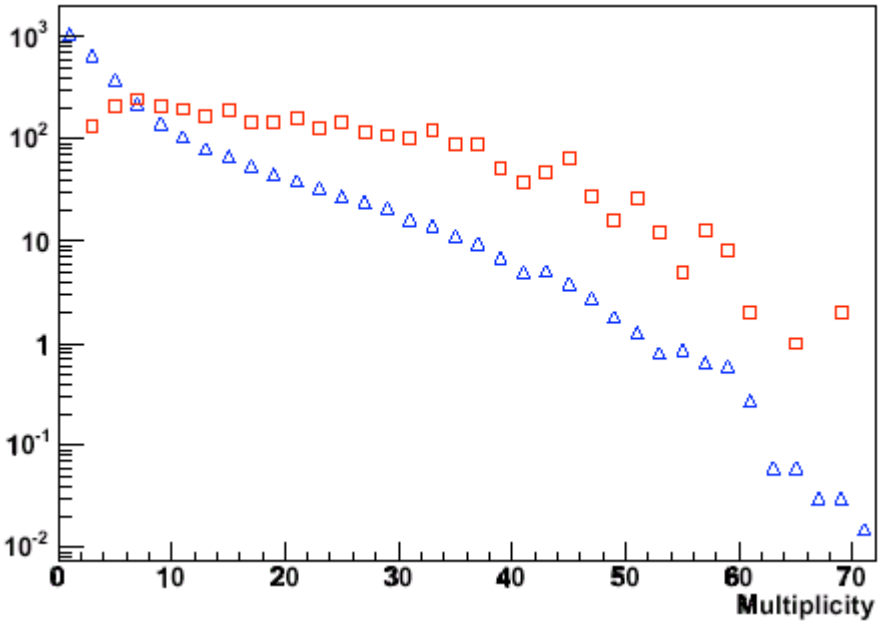

FIG. 18: Pseudorapidity distribution of all kaons generated by PYTHIA (red), compared to that of the kaons produced in a $K^*(892)^0$ decay.

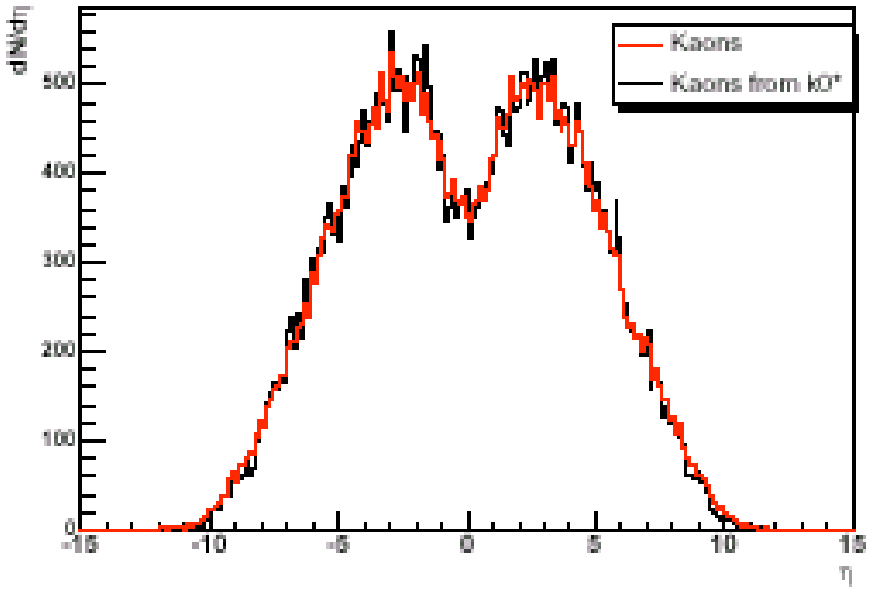

FIG. 19: Multiplicity distribution of all events generated by PYTHIA (blue), compared to the multiplicity distribution of the events containing kaons produced in a $K^*(892)^0$ decay. The two spectra are normalized to the same area.

4.3.2 PID required from ITS, TPC and TOF, Case I

To improve PID, although at the expense of the efficiency, a PID information may be required from each individual ITS, TPC and TOF detector, resulting in a more regular behaviour of the PID efficiency as a function of the particle momenta (See Figs. 20 and 21, for the overall set of kaons and for those kaons originating from the $K^*(892)^0$ decay). For such case the number of reconstructed events was 180000 instead of 200100, as in Case I.

The corresponding numbers are the following: No. of findable $K^*(892)^0$ = 484 (484/180000=0.0027/evt), No. of good anti $K^*(892)^0$ = 460 (460/180000=0.0025/evt)

Considering the interval of invariant mass (0.8,1.0) there are 422 findable $K^*(892)^0$ among 3137 $K^+ \pi^-$ combinations, with a signal to noise ratio = 0.15 and a significance = 7.5. The resulting difference spectrum between the signal and the combinatorial spectrum is reported in Fig.22.

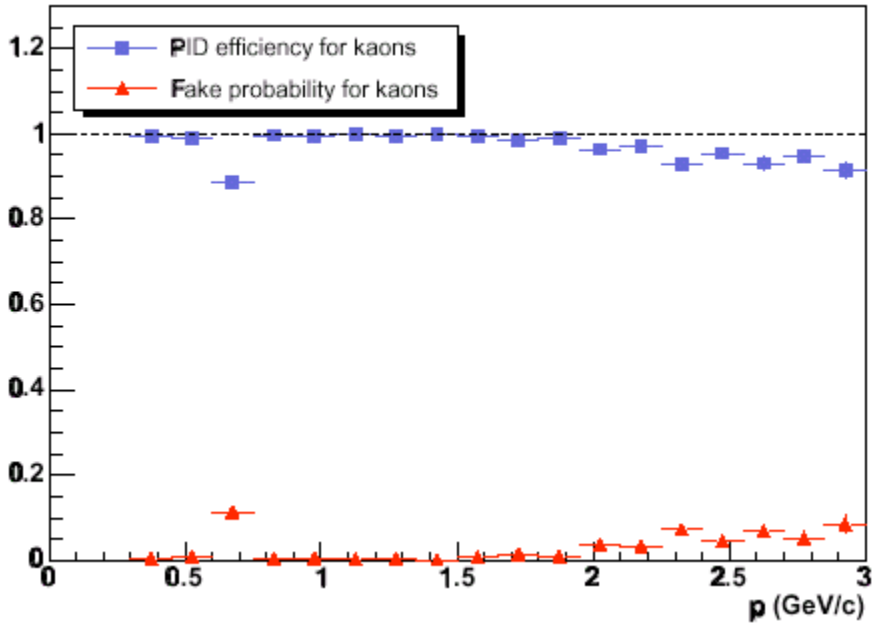

FIG. 20: The two plots show the PID efficiency and the fake probability as a function of the track momentum, for kaons. Particle identification from ITS, TPC and TOF is required.

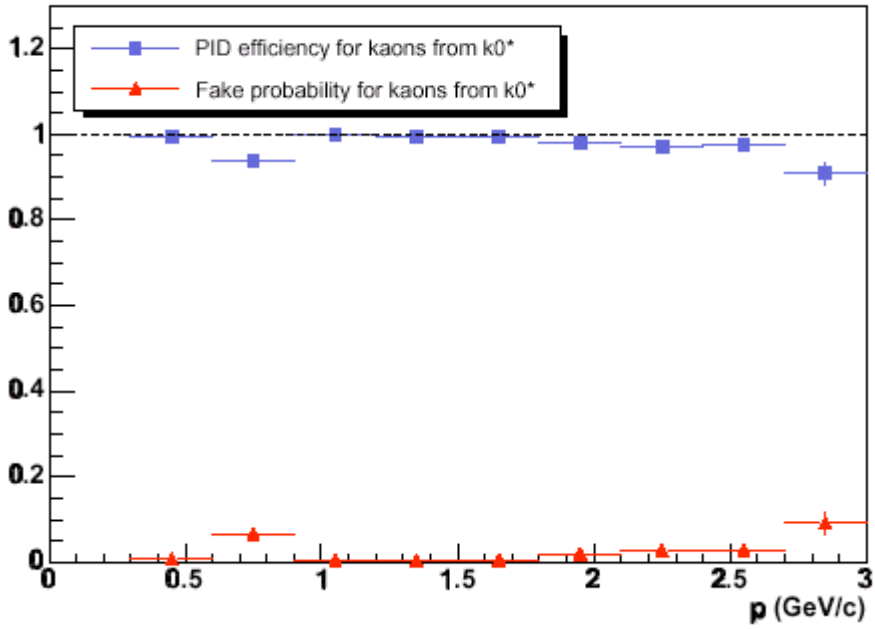

FIG. 21: As Fig.20, for those kaons originating from the decay of $K^*(892)^0$

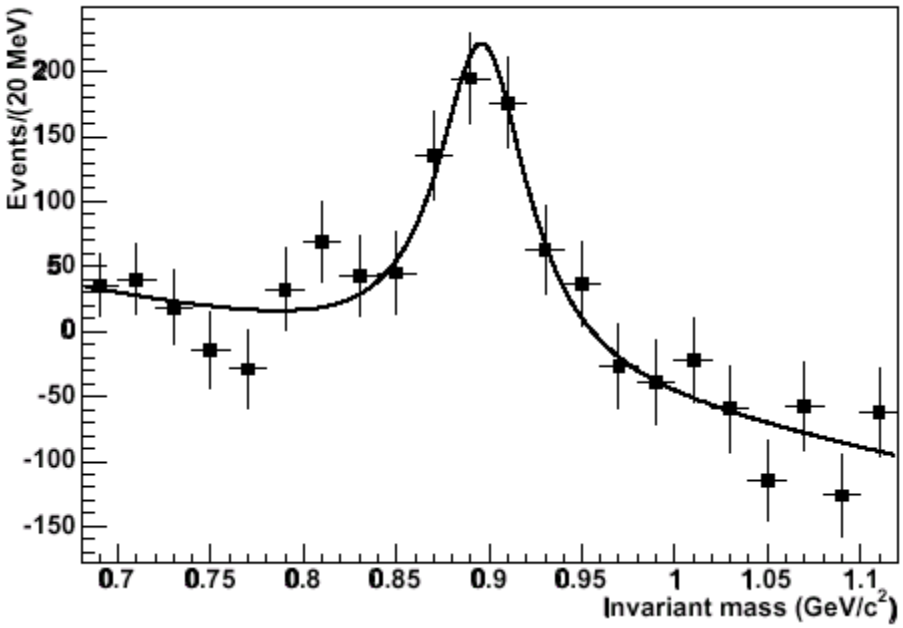

FIG. 22: Subtraction of the K π invariant mass distributions (both the $K^+ \pi^-$ and the $K^- \pi^+$ combinations have been included) and the mixed event background normalized to the same area. The resulting spectrum has been fitted with a Lorentzian curve plus a linear background.

5. CONCLUSIONS

In conclusion, we have carried out a detailed simulation study of the $K^*(892)^0$ and its antiparticle in proton-proton collisions at $\sqrt{s} = 14$ TeV, i.e. at the full energy planned at the future Large Hadron Collider. The reconstruction of the decay products of such resonances has been made by the use of a detailed description of the ALICE detector, with tracking and detection strategies which reflect the present status of development within the Collaboration. Two extreme hypotheses have been considered as far as the correct particle identification inside the detector is concerned. The results show that even in absence of any particle identification, which will not be the case, a realistic analysis of the $K^*(892)^0$ signal may be carried out in pp collisions by a proper evaluation of the combinatorial background with the event mixing technique. Good particle identification, such as can be expected in ALICE by a combined use of the ITS, TPC, TRD and TOF detectors in a large momentum range, allow the results to approach the ideal case, where the extraction of the signal should be feasible with a good knowledge of the strength and width of the resonance parameters.

This will in turn allow physics studies in view of the more challenging situation with the larger particle multiplicity expected from Pb-Pb collisions at 5.5 TeV/A.

6. REFERENCES

(1) A.Badalà et al., Internal Note ALICE-INT-2002-16 (2002).
(2) The ALICE Collaboration, Physics Performance Report, Vol. I, Report CERN-LHCC-2003-049 (2003); J.Phys. G30(2004)1517.
(3) V.Friese for the NA49 Collaboration, Nucl.Phys.A698(2002)487c.
(4) C.Adler et al. (STAR Collaboration), J.Physics G28(2002)1599.
(5) H.Zhang et al., (STAR Collaboration), J.Phys. G30(2004)S577.
(6) A.Badalà et al., Internal Note ALICE-INT-2003-31 (2003).
(7) G.Lo Re et al., Proceedings of the ACAT 2003 Conference; Nuclear Instruments and Methods in Physics Research 533(2004), in press.
(8) http://alien.cern.ch/
(9) http://Alice.web.cern.ch/ALICE/
(10) The ALICE Collaboration, Report LHCC-99-12 (1999).
(11) The ALICE Collaboration, Report LHCC-2000-001 (2000).
(12) The ALICE Collaboration, Report LHCC-2001-021 (2001).
(13) The ALICE Collaboration, Report LHCC-2000-012 (2000), Report LHCC-2002-016 (2002).
(14) The ALICE Collaboration, Report LHCC-1999-22(1999); Report LHCC-2000-046(2000).
(15) http://alisoft.cern.ch/
(16) H.-U. Bengtsson and T.Sjostrand, Comput. Phys. Commun. 46(1987)43; T.Sjostrand, Comput. Phys.Commun. 82(1994)74.
(17) G.Marchesini et al., Comput.Phys.Commun. 67(1992)465.
(18) P.Billoir, Nuclear Instruments and Methods A225(1984)352.
(19) I.Foster and C.Kesselman, Eds.: "The GRID: blueprint for a new computing infrastructure", San Francisco, Morgan Kauffman, 1999.
(20) Particle Data Group, K.Hagiwara et al., Phys. Rev. D66,010001(2002).
(21) J.Podolanski and R.Armenteros, Phil. Mag. 45(1954)13.
(22) D.Drijard, H.G.Fischer and T.Nakada, Nuclear Instruments and Methods A225(1984)367